

Rotationally driven magnetic reconnection in Saturn' dayside

R. L. Guo^{1,2}, Z. H. Yao^{2*}, Y. Wei^{1,11}, L. C. Ray³, I. J. Rae⁴, C. S. Arridge³, A. J. Coates⁴, P. A. Delamere⁵, N. Sergis^{6,12}, P. Kollmann⁷, D. Grodent², W. R. Dunn⁴, J. H. Waite⁸, J. L. Burch⁸, Z. Y. Pu⁹, B. Palmaerts², and M. K. Dougherty¹⁰

1 Key Laboratory of Earth and Planetary Physics, Institute of Geology and Geophysics, Chinese Academy of Sciences, Beijing, China

2 Laboratoire de Physique Atmosphérique et Planétaire, STAR Institute, Université de Liège, Liège, Belgium

3 Department of Physics, Lancaster University, Bailrigg, Lancaster LA1 4YB, UK

4 Mullard Space Science Laboratory, University College London, Holmbury St Mary, Dorking, RH5 6NT, UK

5 University of Alaska Fairbanks, Geophysical Institute, 903 Koyokuk Drive, Fairbanks, AK 99775-7320, USA

6 Office for Space Research and Technology, Academy of Athens, Athens, Greece

7 Applied Physics Laboratory, Johns Hopkins University, Laurel, Maryland, USA

8 Southwest Research Institute, San Antonio, TX, United States

9 School of Earth and Space Sciences, Peking University, Beijing, China

10 Faculty of Natural Sciences, Department of Physics, Imperial College, London, UK

11 College of Earth Sciences, University of Chinese Academy of Sciences, Beijing, China

12 Institute of Astronomy, Astrophysics, Space Applications and Remote Sensing, National Observatory of Athens, Athens

Correspondence to Zhonghua Yao (zhonghua.yao@ulg.ac.be)

Magnetic reconnection is a key process that explosively accelerates charged particles, generating phenomena such as nebular flares¹, solar flares², and stunning aurorae³. In planetary magnetospheres, magnetic reconnection has often been identified on the dayside magnetopause and in the nightside magnetodisc, where thin-current-sheet conditions are conducive to reconnection⁴. The dayside magnetodisc is usually considered thicker than the nightside due to the compression of solar wind, and thus not an ideal environment for reconnection. In contrast, a recent statistical study of magnetic flux circulation strongly suggests that magnetic reconnection must occur throughout Saturn's dayside magnetosphere⁵. Additionally, the source of energetic plasma can be present in

the noon sector of giant planetary magnetospheres⁶. However, so far dayside magnetic reconnection has only been identified at the magnetopause. Here we report the direct evidence of near-noon reconnection within Saturn's magnetodisc using measurements from the Cassini spacecraft. The measured energetic electrons and ions, ranging from tens to hundreds of keV, and the estimated energy flux of $\sim 2.6 \text{ mW/m}^2$ within the reconnection region are sufficient to power aurorae. We suggest that dayside magnetodisc reconnection can explain bursty phenomena in the dayside magnetospheres of giant planets, which can potentially advance our understanding of quasi-periodic injections of relativistic electrons⁶ and auroral pulsations⁷.

Magnetic reconnection plays a crucial role in coupling energy between the solar wind and planetary magnetospheres (e.g., Earth, Mercury, Saturn, Jupiter). The mass and energy circulation at magnetopause and nightside magnetodisc associated with the solar wind is called the 'Dungey cycle'³. In addition to the solar wind influence, the fast rotation of Jupiter and Saturn can also initiate magnetic reconnection and radially outward transport plasmas initially generated by volcanic or tectonic activities of their moons⁸. Magnetic reconnection on the nightside driven by the centrifugal force associated with planetary rotation is known as 'Vasyliunas reconnection'⁸. Moreover, the Kelvin-Helmholtz mode is often unstable on the magnetopause, where viscous-like processes can trigger small-scale and intermittent reconnection, transferring significant momentum⁹ from the solar wind to the magnetosphere. How the three mechanisms compete or cooperate is an open question, and commonly none of them are thought to lead to magnetic reconnection at dayside magnetodisc. For any driver of magnetic reconnection, a reversal of the north-south magnetic component in the plane of the planetary dipole inside the magnetosphere is often adopted as the indicator of reconnection region at both dayside and nightside^{3,5,8,10-13}.

Fig. 1 presents measurements of magnetic fields from the Cassini-MAG instrument¹⁴ and plasma from the Cassini-CAPS instrument¹⁵. The magnetic fields are in Kronographic Radial-Theta-Phi (KRTP) coordinates. Clear magnetopause crossings were observed at $\sim 19 R_S$ (Radius of Saturn, $1 R_S = 60,268 \text{ km}$) on September 27, 2008 (indicated by the black arrows at the bottom of the figure). On September 30 at $\sim 08:40 \text{ UT}$ (pink-shaded area), there was a significant negative B_θ event accompanied by an enhancement of electron flux with energies up to tens of keV, which we later demonstrate is a signature of magnetic reconnection. The event was measured at $\sim 17.5 R_S$, which is about $1.5 R_S$ planetward of the magnetopause encountered earlier in that interval.

We detail this negative B_θ event in Fig. 2. The magnetic field vectors have been transformed into the X-line coordinate system as described in Arridge, et al.¹². This coordinate system has previously been used¹² to clearly show the Hall magnetic field (shown as quadrupolar magnetic field in the 2D slice of the reconnection region, see

Fig. 3) associated with a Hall current system¹⁶. The quadrupolar magnetic field projection onto the Cassini spacecraft trajectory (shown in Fig. 3 and Supplementary Figure 1) is a bipolar signature, which is a key piece of evidence of a reconnection process^{12,16} (note that another piece of key evidence is reconnection accelerated electron distributions, which will later be detailed in this letter). Accompanying the B_Y reversal, B_Z turned from northward (~ 2 nT) to southward (~ -2 nT). The “northward to southward” turning suggests that the Cassini spacecraft travelled from the outward reconnection site (i.e., Sunward of this event) to the planetary side, as we have illustrated in Fig. 3.

This reconnection event has also produced substantial energization of the charged particles. It is clear that energetic ions (up to 300 keV) and electrons (10s -100 keV) are detected in the reconnection ion diffusion region around 08:43 UT (Fig. 2d and 2f, measurements from the MIMI-LEMMS instrument¹⁷). In addition, very energetic O^+ up to ~ 590 keV has also been detected in this region, suggesting that this reconnection process can efficiently produce very energetic heavy ions (see Supplementary Figure 2). The existence of the heavy ions might imply that the internally driven process take place.

The energetic ions were detected at the Sunward reconnection site ($B_Z > 0$). Interestingly, peak intensities of energetic electrons were detected later in the region of $B_Z < 0$, suggesting that the region of $B_Z > 0$ is not the most efficient electron acceleration site. The sudden enhancement of B_X and decrease of B_Z during $B_Y > 0$, along with the simultaneously significant decrease of the fluxes of both energetic ions and electrons recorded by MIMI-LEMMS, indicates a rapid variation of the reconnection site (i.e., localised structure, or vertical current sheet oscillation, details are provided in Method section). Coinciding with the sign reversal of B_Y , Cassini entered the planetary side of the X-line ($B_Z < 0$). The smaller value of B_X indicates that the spacecraft was closer to the current center than when it encountered the Sunward reconnection site (details are shown in Method section). The measured increase in the flux of energetic electrons also implies that the spacecraft moved closer to the X-line and had crossed the electron edge to enter the electron exhaust region¹⁸, where electrons were significantly heated. The energetic electrons and ions are both observed first at low energies, followed by higher energies, indicating that they were not injected from distant place (Note that the ions and electrons would show inverse energy time dispersion feature in injection events¹⁹). These features are remarkably similar to the reconnection event observed at Earth’s magnetotail reported in Angelopoulos, et al.¹¹.

An inferred trajectory of Cassini in the reconnection diffusion region and the measured electron pitch angle distributions are presented in Fig. 3. During a reconnection event, the inflowing ambient electron population and the outflowing accelerated electrons are frozen-in to magnetic field lines either inside or outside the diffusion region¹⁶. Therefore, electron distribution information is often adopted

as direct evidence for identifying a reconnection site. The three pitch-angle vs. energy distributions at the bottom of Fig. 3 represent (from left to right) populations from the background environment, Sunward of the X-line, and planetward of the X-line. Each distribution is obtained by averaging all data over the selected durations (indicated at the top of each distribution plot) in the selected region. The bi-streaming thermal electrons (fluxes with dominant pitch angle distributions at 0 and 180 degrees, i.e. parallel and antiparallel to the magnetic field vector) in both the Sunward and planetward directions suggest that the magnetic field was not open to the interplanetary medium on either side of the reconnection site, which implies that the reconnection was driven by an internal process, i.e., the rotation of the planet. In addition to the bi-streaming feature of the thermal electrons, the pitch angle distributions on both sides of the X-line show clear asymmetries. At the Sunward reconnection site, the energy flux of the parallel population was significantly larger than the antiparallel population. Contrary to the Sunward population, the planetward population was dominated by an antiparallel population. The higher fluxes were also at higher energies, suggesting an acceleration process. As shown in the sketch of Fig. 3, the parallel direction on the Sunward reconnection site and antiparallel direction on planetward reconnection site both represent directions away from the X-line, strongly evidencing that Cassini was measuring an ongoing rotationally driven magnetospheric reconnection process at near-noon local time. The enhancement of the perpendicular population in the planetward reconnection site again indicates that the Cassini spacecraft went into the electron exhaust region close to the X-line, where the perpendicular electron heating is naturally expected²⁰.

To distinguish from magnetopause reconnection, we henceforth refer to this reconnection event as “dayside magnetodisc reconnection” (DMDR). A dimensionless reconnection rate (i.e., the ratio between reconnection inflow velocity and Alfvén speed) is estimated by the quantity $|B_z|/|B_x|$ ¹², from which we obtain a reconnection rate of ~ 0.3 , which is of the order predicted by the fast Hall reconnection model²¹. As illustrated in the Method section, the energy precipitation from this reconnection event ($\sim 2.6 \text{ mW/m}^2$) would produce an intermediate aurora emission with intensity up to 26 kR.

In-situ evidence of magnetic reconnection in the noon sector of Saturn’s magnetosphere is important to planetary, plasma, and magnetospheric science at least in the following aspects: First, the existence of reconnection in the noon sector of a magnetosphere would require an update of magnetospheric convection models. The magnetosphere is compressed by the solar wind, which causes the bulging of field lines towards high latitudes. As a consequence, it is generally assumed that reconnection cannot exist well-inside the magnetopause. The existence of DMDR in the noon sector requires a reconsideration of the balance between internally and

solar wind driven processes in controlling magnetic reconnection. It is possible that the former can sometimes dominate the latter even on the dayside. Second, direct observations of accelerated electrons from the reconnection site provide a new fundamental explanation for previously measured energetic electrons²² in the outer parts of the dayside magnetosphere. Third, dayside auroral pulsations^{23,25,26} can be explained by such a mechanism. Dayside auroral emissions are particularly prominent phenomena at both Saturn and Jupiter and previously have been suggested to be triggered by magnetic reconnection at the magnetopause^{23,24}. There are two types of auroral emissions at Saturn's dayside polar region: local time-fixed aurora, and corotating/subcorotating aurora. The solar wind interaction generally controls magnetopause reconnection, thus the X-line is not expected to co-rotate with the planet, i.e., remains local time-fixed. Sub-corotating auroral pulsations have been reported on the dayside of the planet⁷. However, they cannot be fully explained by the magnetopause reconnection. The DMDR could possibly co-rotate with the planet, and thus may explain the origin for rotating auroral pulsations. Fourth, magnetic reconnection can directly accelerate electrons up to a few keV to tens of keV in planetary magnetospheres, providing an important particle source to generate auroral pulsations at Saturn²⁵ and Jupiter²⁶. The hundreds of keV ions observed in this reconnection event imply that the existence of such high-energy ions in giant magnetospheres can be explained by DMDR. If a similar DMDR process operates in the Jovian dayside magnetodisc then this may explain the pulses of UV and X-ray emissions in Jupiter's polar region²⁷.

Furthermore, the counterpart of auroral pulsations, quasi-periodic enhancements of energetic electrons (QP60 events)^{6,22}, were observed to occur during the reconnection event and lasted for more than 14 hours (see Supplementary Figure 5). DMDR could thus provide a potential explanation for the still poorly understood QP60 events in Saturn's magnetosphere, occurring when the reconnection process is unsteady and the reconnection rate changes periodically²⁸.

The mass loss rate estimated from plasmoid down-tail release in previous studies is not sufficient to balance the loading rate contributed by Saturn's satellites⁵. Long duration magnetic reconnection in the magnetotail¹² and drizzle-like reconnection sites in the afternoon and night sectors⁵ have been proposed to accelerate/increase the total loss process. The DMDR could support the drizzle-like reconnection picture, which enables internally driven dynamics to lead to loss processes on the dayside⁵, and by extension, throughout the whole magnetosphere.

DMDR may play a fundamental role in the transport and energisation processes of all rapidly rotating magnetospheres. The extent to which this process is important at Jupiter and Saturn remains to be determined, which urges the importance to revisit the dataset from previous giant planetary missions (e.g., Cassini and Galileo) and the current Juno spacecraft.

References

- 1 Clausen-Brown, E. & Lyutikov, M. Crab nebula gamma-ray flares as relativistic reconnection minijets. *Monthly Notices of the Royal Astronomical Society* **426**, 1374-1384 (2012).
- 2 Parker, E. N. The Solar-Flare Phenomenon and the Theory of Reconnection and Annihilation of Magnetic Fields. *The Astrophysical Journal Supplement Series* **8**, 177 (1963).
- 3 Dungey, J. W. Interplanetary magnetic field and the auroral zones. *Physical Review Letters* **6**, 47 (1961).
- 4 Paschmann, G. *et al.* Plasma acceleration at the Earth's magnetopause: evidence for reconnection. *Nature* **282**, 243-246 (1979).
- 5 Delamere, P., Otto, A., Ma, X., Bagenal, F. & Wilson, R. Magnetic flux circulation in the rotationally driven giant magnetospheres. *Journal of Geophysical Research: Space Physics* **120**, 4229-4245 (2015).
- 6 Roussos, E. *et al.* Quasi-periodic injections of relativistic electrons in Saturn's outer magnetosphere. *Icarus* **263**, 101-116 (2016).
- 7 Mitchell, D. *et al.* Recurrent pulsations in Saturn's high latitude magnetosphere. *Icarus* **263**, 94-100 (2016).
- 8 Vasyliunas, V. Plasma distribution and flow. *Physics of the Jovian magnetosphere* **1**, 395-453 (1983).
- 9 Burkholder, B. *et al.* Local time asymmetry of Saturn's magnetosheath flows. *Geophysical Research Letters* **44**, 5877-5883, doi:10.1002/2017GL073031 (2017).
- 10 Yao, Z. *et al.* Corotating Magnetic Reconnection Site in Saturn's Magnetosphere. *The Astrophysical Journal Letters* **846**, doi:10.3847/2041-8213/aa88af (2017).
- 11 Angelopoulos, V. *et al.* Tail reconnection triggering substorm onset. *Science* **321**, 931-935, doi:10.1126/science.1160495 (2008).
- 12 Arridge, C. S. *et al.* Cassini in situ observations of long-duration magnetic reconnection in Saturn's magnetotail. *Nature Physics*, 268-271 (2016).
- 13 Kronberg, E., Kasahara, S., Krupp, N. & Woch, J. Field-aligned beams and reconnection in the jovian magnetotail. *Icarus* **217**, 55-65 (2012).
- 14 Dougherty, M. K. *et al.* The Cassini Magnetic Field Investigation. *Space Science Reviews* **114**, 331-383, doi:10.1007/s11214-004-1432-2 (2004).
- 15 Young, D. *et al.* Cassini Plasma Spectrometer Investigation. *Space Science Reviews* **114**, 1-112 (2004).
- 16 Nagai, T. *et al.* Geotail observations of the Hall current system: Evidence of magnetic reconnection in the magnetotail. *Journal of Geophysical Research: Space Physics* **106**, 25929-25949 (2001).

- 17 Krimigis, S. *et al.* in *The Cassini-Huygens Mission* 233-329 (Springer, 2004).
- 18 Lindstedt, T. *et al.* in *Ann Geophys-Germany*. 4039-4056 (Copernicus GmbH).
- 19 Mauk, B. *et al.* Transient aurora on Jupiter from injections of magnetospheric electrons. *Nature* **415**, 1003 (2002).
- 20 Wang, S. *et al.* Electron heating in the exhaust of magnetic reconnection with negligible guide field. *Journal of Geophysical Research: Space Physics* **121**, 2104-2130, doi:10.1002/2015ja021892 (2016).
- 21 Birn, J. *et al.* Geospace Environmental Modeling (GEM) magnetic reconnection challenge. *Journal of Geophysical Research: Space Physics* **106**, 3715-3719 (2001).
- 22 Palmaerts, B. *et al.* Statistical analysis and multi-instrument overview of the quasi-periodic 1-hour pulsations in Saturn's outer magnetosphere. *Icarus* **271**, 1-18 (2016).
- 23 Radioti, A. *et al.* Auroral signatures of multiple magnetopause reconnection at Saturn. *Geophysical Research Letters* **40**, 4498-4502 (2013).
- 24 Badman, S. V. *et al.* Bursty magnetic reconnection at Saturn's magnetopause. *Geophysical Research Letters* **40**, 1027-1031, doi:10.1002/grl.50199 (2013).
- 25 Gérard, J. C. *et al.* Altitude of Saturn's aurora and its implications for the characteristic energy of precipitated electrons. *Geophysical Research Letters* **36**, L02202, doi:10.1029/2008GL036554 (2009).
- 26 Grodent, D., Gérard, J. C., Clarke, J., Gladstone, G. & Waite, J. A possible auroral signature of a magnetotail reconnection process on Jupiter. *Journal of Geophysical Research: Space Physics* **109** (2004).
- 27 Gladstone, G. *et al.* A pulsating auroral X-ray hot spot on Jupiter. *Nature* **415**, 1000-1003 (2002).
- 28 Fu, H. S., Khotyaintsev, Y. V., Vaivads, A., Retino, A. & Andre, M. Energetic electron acceleration by unsteady magnetic reconnection. *Nature Physics* **9**, 426-430, doi:10.1038/Nphys2664 (2013).

Correspondence and requests for materials should be addressed to Z.H.Y.

Acknowledgement: The work was supported by the National Science Foundation of China (41525016, 41474155, 41704169, 41274167). Z.H.Y. is a Marie-Curie COFUND research fellow, cofunded by EU. Cassini operations are supported by NASA (managed by the Jet Propulsion Laboratory) and ESA. R.L.G. is supported by opening fund of Lunar and Planetary Science Laboratory, MUST-Partner Laboratory of Key Laboratory of Lunar and Deep Space Exploration, CAS (Macau FDCT grant No. 039/2013/A2). I.J.R. is supported in part by STFC grant ST/N000722/1. Z.H.Y, B.P and D.G. are supported by the PRODEX program managed by ESA in collaboration with the Belgian Federal Science Policy Office. W.R.D. is supported by a Science and Technology Facilities Council (STFC) research grant to University College London

(UCL), an SAO fellowship to Harvard-Smithsonian Centre for Astrophysics and by European Space Agency (ESA) contract no. 4000120752/17/NL/MH. AJC is supported by a UK Science and Technology Facilities Council (STFC) Consolidated Grants to UCL-MSSL (ST/K000977/1 and ST/N000722/1).

Author Contributions:

All authors were involved in the writing of the paper. R.L.G., Z.H.Y. and Y.W. led the work and conducted most of the analysis for Cassini measurements. L.C.R. provided knowledge of planetary magnetospheric dynamics and critical review of the techniques applied, along with extensive paper writing and data analysis. I.J.R., C.S.A., P.A.D. Z. P. and J.L.B. provided expertise on auroral drivers, magnetospheric processes. N.S. and P.K. provided crucial support in using ion data, and insight in magnetospheric dynamics. A.J.C., D.G., W.R.D., J.H.W., B.P. and M.K.D. provided detailed knowledge of planetary magnetospheres.

Figures

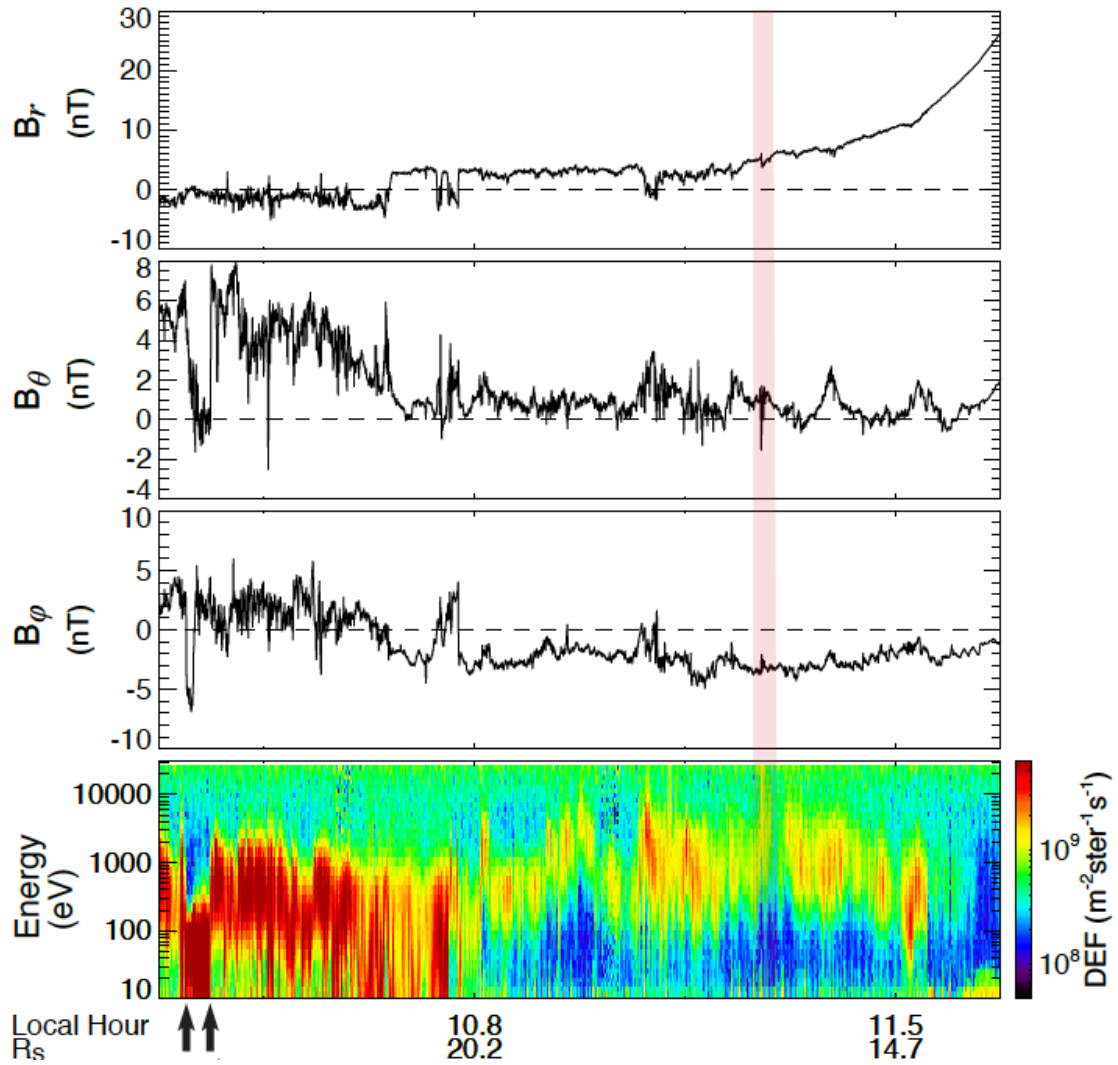


Fig. 1: Overview of the magnetopause and dayside magnetosphere crossing near the magnetic reconnection event on 30 Sep 2008. The first three panels are the three components of magnetic field in KRTP coordinate (a spherical coordinate system whose z-axis is Saturn's rotation axis pointing to north), i.e. B_r , B_θ , B_ϕ . The bottom panel is the electron differential energy flux from Cassini/CAPS-ELS instrument. The pink-shaded area marks the magnetic reconnection event. Black arrows indicate magnetopause crossings. From 29 Sep to 01 Oct, Cassini was well inside the magnetosphere, and measures the magnetospheric electron population with energies from few hundreds to thousands eV.

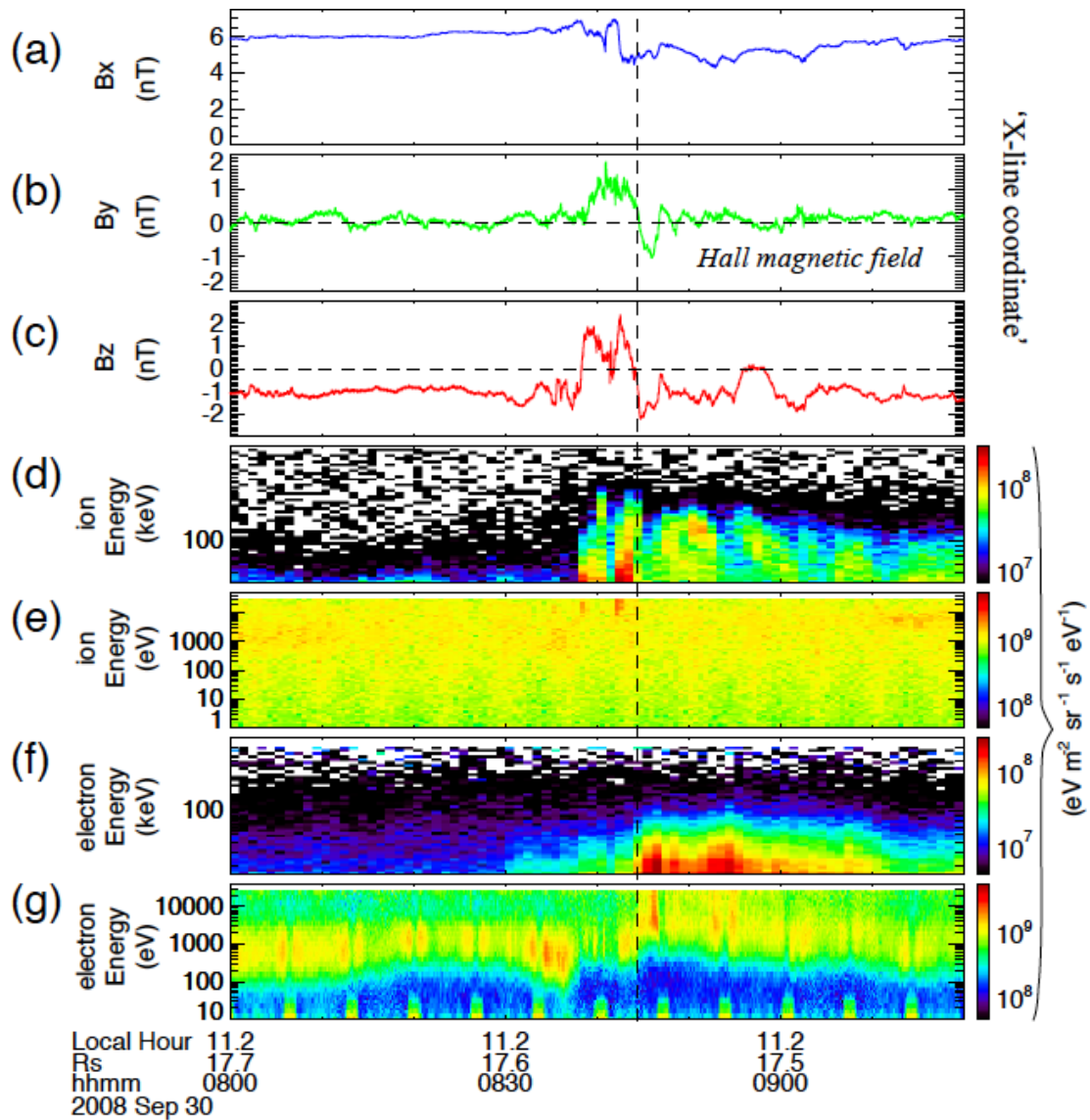


Fig. 2: Magnetic and plasma measurements in the magnetic reconnection region. (a-c) three components of the magnetic field vectors in X-line coordinate as described in Arridge, et al. ¹². (d and e) Differential energy fluxes of ions with energies from 25 keV to 781 keV measured by the MIMI instrument (LEMMS PHA_A channels, which measure total ions but are dominated by protons), and energies up to 46 keV measured by CAPS-IMS¹⁵ instrument. (f and g) Differential energy fluxes of electrons with energies from 20 keV to 423 keV measured by the MIMI-LEMMS instrument, and energies up to 26 keV measured by CAPS-ELS instrument (red stripes at 10s of eV is not real due to photoelectrons). The vertical dashed line indicates the reversal of B_y and B_z .

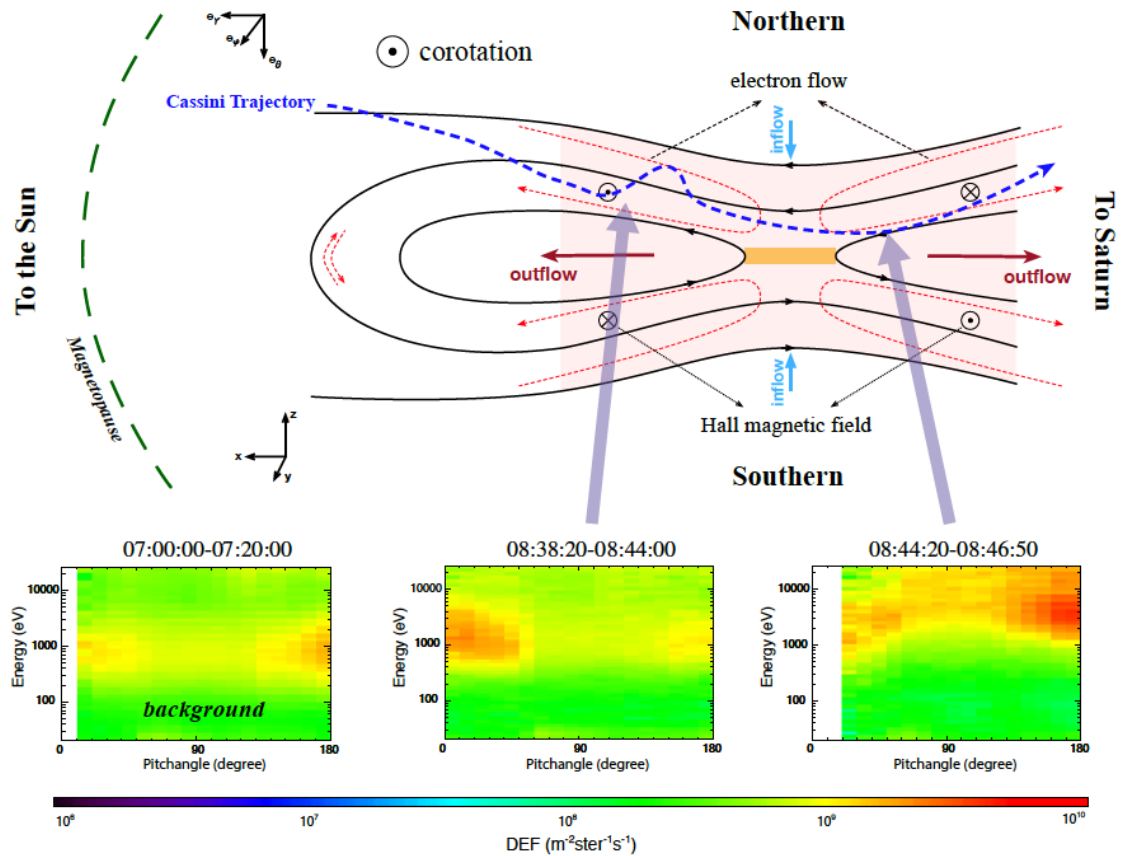


Fig. 3: The trajectory of Cassini relative to the geometry of the reconnection diffusion region and detected electron pitch angle distribution at different regions. Top: sketch of the geometry of the reconnection diffusion region (The large-scale magnetospheric context is displayed in Supplementary Figure 6). Black curves are field lines and the arrows are the directions. The shallow pink and deep yellow regions are the ion and electron diffusion regions. The red dashed curves with arrows show the movements of electrons around the separatrix. The magnetopause is at the left and is presented by the green dashed curve. The potential trajectory of Cassini is indicated by the blue dashed curves. **Bottom:** From left to right, electron pitch angle-energy distributions from background environment (i.e., outside reconnection region), outward of X-line and planetary side of X-line. The x-axis of each plot is the pitch angle and the y-axis is energy.

Methods:

Cassini position and the location of magnetopause

Supplementary Figure 1 shows the position of the Cassini spacecraft in the Kronocentric Solar Magnetospheric Coordinates (KSM). The thick black curve represents the modeled magnetopause from the A60 model²⁹, while the solar wind parameter is given by the Tao solar wind propagation model³⁰. Blue curves are the inner and outer boundary of the predicted magnetopause accounting for the errors of the parameters in the modeling²⁹. The red dot indicates the position of the spacecraft for the measurements of the event in this paper. Clearly, the spacecraft was located inside the magnetopause, consistent with the Cassini measurements shown in Fig. 1.

Though Cassini's latitude is high (~29 degrees), the current sheet can oscillate with large amplitudes within durations much less than the rotation period (~10 h) to arrive at the Cassini spacecraft. The overview plot in Figure 1 also shows such large oscillations of the current sheet at ~20:00 UT on September 29, where the spacecraft crossed the center of the current sheet (B_r turned to negative) while Cassini's latitude is around 22 degrees. This kind of large vertical oscillation could be a combination of several effects. During this period, the current sheet should be warped/displaced northwards by around 1 R_s to form a bowl-shape³¹. Some models and studies show oscillatory (~10 h) motion of the sheet in the magnetotail³², which might be expected in the noon sector. Another important effect is the dynamical vertical/flapping motion (minutes to hours) of the current sheet. The dynamical motion of the current sheet is also very common in Earth's magnetosphere, especially when reconnection and substorms take place^{33,34}. The B_r component of the magnetic field observed by Cassini also exhibits similar oscillatory motion with durations much less than the rotation period (such as the oscillation at ~20:00 UT on September 29). As suggested by previous literature, the high latitude current sheet in the outer magnetosphere could be possibly be caused by perturbation from Kelvin-Helmholtz instabilities at the magnetopause^{35,36}.

Explanation of the sudden decrease of energetic particle flux

There exists a significantly low flux (gap) of the energetic ion flux in Fig. 2d when $B_y > 0$. Under certain conditions, a gap in an energy spectrum might be caused by LEMMS and CAPS sampling different directions as a function of time. However, in this study, this is not the case. CAPS-IMS covered a large pitch angle range. Supplementary Figure 3 shows the differential energy flux detected by different anodes, i.e., different directions. The enhancements are at the same time for all anodes. If the enhancement were a temporal effect owing to the variation of the angle between instrument sampling direction and magnetic field vector, then the gap would be present at different times as each instrument's anode pointed towards the proper direction. Furthermore, the gaps are observed both at the same time for ions and

electrons, which is more likely caused when the spacecraft has a relative motion to a structure.

To explain the gap, we suggest that the spacecraft either observed a localised structure featured with strong B_x and depleted energetic plasma (i.e., decrease of fluxes of both energetic ions and electrons by MIMI-LEMMS), or move away from the reconnection site and rapidly return back (e.g., experienced a rapid vertical current sheet oscillation).

For the former one, small-scale structures can exist in the complex reconnection region. The reconnection site could possibly co-rotate with the planet, and thus the spacecraft could cross the reconnection site in the azimuthal direction. The small localised structure can be encountered by spacecraft when co-rotating with the reconnection site, and lead to rapid change of the physical parameters and complex detailed features on plasma characteristics such as the energy dispersion when environment changes in the azimuthal direction.

For the latter one, the vertical oscillation of the current sheet can frequently occur in the dynamical reconnection region. The flux gap was accompanied by a B_x enhancement and B_z decrease, which is always treated as a typical signature of the relative motion of the spacecraft, i.e., moving from the current sheet center to the boundary³⁴. The oscillation of the current sheet is common phenomenon when the magnetosphere is much dynamic. Therefore, when drawing the trajectory of the Cassini spacecraft, we treated the oscillation of the current sheet as the probable scenario.

Relative location between Cassini and the X-line

The region where electrons get accelerated is inside (both in z /vertical and x /transverse directions) the region where ions get accelerated (see Supplementary Figure 4). The center of the reconnection region is called the X-line. The strongest energized ion fluxes appear farther from the X-line than the energized electron fluxes. This can occur because electrons are largely accelerated in electron diffusion region (EDR) around the X-line and in the electron outflow region and electron exhaust region adjacent to the EDR, while ions are accelerated downstream of the electron outflow region. Along the trajectory of Cassini spacecraft (dashed blue curve in Fig. 3), we would thus observe a peak ion flux before electrons, and they are separated by B_y and B_z reversals. Depending on the relative trajectories, different features would also be possible, for example, along trajectory A (red solid line), a spacecraft would observe a reversal of B_x . Regarding the dynamic nature of reconnection process, it is possible to observe many very different features for the same reconnection picture depending on the trajectory of the spacecraft relative to the location of the event. Moreover, the participation of heavy ions could enlarge

the ion diffusion region, and thus the Hall magnetic fields would become more detectable for the spacecraft.

Estimation of the energy release from the magnetic reconnection process

Based on the Sweet-Parker reconnection model^{37,38}, the energy released from the magnetic field can be simply estimated by calculating the difference between the inflowing magnetic energy flux and the outflowing magnetic energy flux. This estimation method can be applied to the Hall reconnection model, as it is based on the energy conservation condition.

The physical parameters of the reconnection region in this letter are: magnetic strength B is 7.07 nT, maximum $|B_x|$ is 6.97 nT, maximum $|B_z|$ is 2.33 nT, the density n is 0.0066 cm⁻³. The density is the electron density obtained from CAPS-ELS, which is equal to the ion density assuming charge neutrality. The proton density is similar to the density of water group at $\sim 17 R_S$ ³⁹. The Alfvén speed is $V_A = B/\sqrt{\mu_0 n m_i} \approx 601$ km/s, where μ_0 is the vacuum permeability, m_i is the averaged ion mass equal $Z m_p$, while m_p is proton mass and Z is ~ 10 (the whole ion population contains half H⁺ with $m/q = 1$ and half water group comprising O⁺, OH⁺, H₂O⁺, and H₃O⁺, with m/q from 16 to 19³⁹). Following Arridge et al.¹², the reconnection rate R is roughly estimated by the quantity $R = |B_z|/|B_x| \sim 0.33$. The outflow speed V_{out} approaches the Alfvén speed, and the inflow speed is $V_{in} = R V_A$ ^{37,38}. The energy flux going into the reconnection region is $W_{in} = (E \times H)_{in} = V_{in} B_{in}^2 / \mu_0 = R V_A B^2 / \mu_0 \approx 0.0079$ mW/m². The outgoing energy flux from the reconnection region is $W_{out} = (E \times H)_{out} = V_{out} B_{out}^2 / \mu_0 = V_A B_z^2 / \mu_0 \approx 0.0026$ mW/m². The flux of energy released from the reconnection event is $P_{release} = P_{in} - P_{out} = 0.0053$ mW/m². Following a simple rule of energy partition in reconnection, half of the energy is transferred to thermal energy⁴⁰, i.e., 0.0027 mW/m².

The altitude of maximum auroral brightness at the ionosphere is $\sim 1,100$ km²⁵, where the averaged magnetic strength is $\sim 68,360$ nT for the north ionosphere⁴¹. Based on the Liouville's theorem, the particle energy flux is proportional to magnetic strength along the magnetic tube⁴¹. That is to say, in the auroral region, the particle energy flux is ~ 25.6 mW/m². Assuming that 10% of the energy can precipitate into the ionosphere to generate aurora, i.e., 2.6 mW/m², which can cause an intermediate aurora emission with intensity up to 26 kR⁴².

The water group ions are dominant only within the equatorial plane³⁹. At later stages, when reconnection moves to slightly higher latitudes, the Alfvén speed will increase due to the dominant species becoming protons. As a consequence, the energy flux

generated by reconnection process will increase, and the associated auroral spot will become brighter with a larger intensity.

Data Availability Statement:

The data that support the plots within this paper and other findings of this study are publicly available from NASA's planetary data system <https://pds-ppi.igpp.ucla.edu/>.

References in the Methods:

- 29 Kanani, S. J. *et al.* A new form of Saturn's magnetopause using a dynamic pressure balance model, based on in situ, multi-instrument Cassini measurements. *Journal of Geophysical Research: Space Physics* **115**, A06207, doi:10.1029/2009ja014262 (2010).
- 30 Tao, C., Kataoka, R., Fukunishi, H., Takahashi, Y. & Yokoyama, T. Magnetic field variations in the Jovian magnetotail induced by solar wind dynamic pressure enhancements. *Journal of Geophysical Research* **110**, doi:10.1029/2004ja010959 (2005).
- 31 Arridge, C. *et al.* Saturn's magnetodisc current sheet. *Journal of Geophysical Research: Space Physics* **113**, A04214, doi:10.1029/2007JA012540 (2008).
- 32 Arridge, C. S. *et al.* Periodic motion of Saturn's nightside plasma sheet. *Journal of Geophysical Research: Space Physics* **116**, A11205, doi:10.1029/2011JA016827 (2011).
- 33 Sergeev, V. *et al.* Current sheet flapping motion and structure observed by Cluster. *Geophysical Research Letters* **30**, 1327-1324, doi:10.1029/2002GL016500 (2003).
- 34 Runov, A. *et al.* Electric current and magnetic field geometry in flapping magnetotail current sheets. *Ann. Geophys.* **23**, 1391-1403, doi:10.5194/angeo-23-1391-2005 (2005).
- 35 Delamere, P. A., Wilson, R. J. & Masters, A. Kelvin-Helmholtz instability at Saturn's magnetopause: Hybrid simulations. *Journal of Geophysical Research: Space Physics* **116**, A10222, doi:doi:10.1029/2011JA016724 (2011).
- 36 Masters, A. *et al.* Cassini observations of a Kelvin-Helmholtz vortex in Saturn's outer magnetosphere. *Journal of Geophysical Research: Space Physics* **115**, A07225, doi:10.1029/2010JA015351 (2010).
- 37 Sweet, P. A. The production of high energy particles in solar flares. *Il Nuovo Cimento (1955-1965)* **8**, 188-196, doi:10.1007/bf02962520 (1958).
- 38 Parker, E. N. Sweet's mechanism for merging magnetic fields in conducting fluids. *Journal of Geophysical Research* **62**, 509-520, doi:10.1029/JZ062i004p00509 (1957).

- 39 Thomsen, M. F. *et al.* Survey of ion plasma parameters in Saturn's magnetosphere. *Journal of Geophysical Research: Space Physics* **115**, A10220, doi:10.1029/2010JA015267 (2010).
- 40 Korovinskiy, D. B., Semenov, V. S., Erkaev, N. V., Divin, A. V. & Biernat, H. K. The 2.5-D analytical model of steady-state Hall magnetic reconnection. *Journal of Geophysical Research: Space Physics* **113**, A04205, doi:10.1029/2007JA012852 (2008).
- 41 Nichols, J. D. *et al.* Saturn's equinoctial auroras. *Geophysical Research Letters* **36**, L24102, doi:10.1029/2009GL041491 (2009).
- 42 Yao, Z. H. *et al.* Mechanisms of Saturn's Near-Noon Transient Aurora: In Situ Evidence From Cassini Measurements. *Geophysical Research Letters* **44**, 217-228, doi:10.1002/2017GL075108 (2017).